Study of Impurity Transport in Deuterium and Hydrogen Plasmas in the Edge Stochastic Magnetic Field Layer of Large Helical Device

T. Oishi[1,2], S. Morita[1,2], M. Kobayashi[1,2], G. Kawamura[1,2], Y. Kawamoto[1], M. Goto[1,2] and the LHD Experiment Group[1]

[1] *National Institute for Fusion Science, National Institutes of Natural Sciences, 322-6, Oroshi-cho, Toki, Gifu 509-5292, Japan*

[2] *Department of Fusion Science, SOKENDAI (Graduate University for Advanced Studies), 322-6, Oroshi-cho, Toki, Gifu 509-5292, Japan*

Stochastization of edge magnetic fields is extensively studied not only for the ELM mitigation but also for the plasma detachment and the impurity transport. A thick stochastic magnetic field layer called "ergodic layer" of the large helical device (LHD) consists of stochastic magnetic fields with three-dimensional structure intrinsically formed by helical coils, while well-defined magnetic surfaces exist inside the last closed flux surface [1]. It is therefore extremely important to study the impurity behavior and transport in the ergodic layer and to compare with those in the scrape-off layer of tokamaks. In LHD, it is found that carbon impurities are screened by the presence of the ergodic layer [2] and iron impurities are more effectively screened. As a result, the iron density in core plasmas of LHD is found to be extremely low despite the stainless steel vacuum vessel [3]. A transport model for the impurity behavior in the ergodic layer has been proposed considering the parallel momentum balance on impurity ions along a magnetic field line connecting the core plasma and the divertor plate based on the following equation;

$$m_Z \frac{\partial V_{Z//}}{\partial t} = -\frac{1}{n_Z}\frac{\partial T_Z n_Z}{\partial s} + ZeE_{//} + m_Z \frac{V_{i//} - V_{Z//}^{imp}}{\tau_s} + 0.71Z^2 \frac{\partial T_e}{\partial s} + 2.6Z^2 \frac{\partial T_i}{\partial s}, \quad (1)$$

where five terms in the right-hand side are contributions of impurity ion pressure gradient, parallel electric field, friction force between bulk ions and impurity ions, electron thermal force, and ion thermal force, in the order [4]. Among these terms, the friction force term and the ion thermal force term are the dominant terms. When the ion density gradient increases, the friction force increase resulting the impurity flow is directed toward divertor plates, which means the impurity screening. On the other hand, when the ion temperature gradient increases, the ion thermal force increases resulting that the impurity flow is directed toward the core plasmas, which means the impurity accumulation. Based on the model, the parallel flow of the impurity ions is considered to be a key mechanism to determine impurity distributions in the ergodic layer.

In the present study, spectroscopic diagnostics has been performed in discharges with a magnetic configuration with the position of the magnetic axis, R_{ax}, of 3.6 m and the toroidal magnetic field, B_t, of 2.75 T. The discharge initiated by the electron cyclotron heating (ECH) is grown by three neutral beam injections based on the negative ion sources (n-NBI) beams with total port-through power of 10 MW and maintained with a flat-top phase for 1 s. We performed similar operations for the working gas of H_2 and the beam particle of the neutral beam of hydrogen (denoted as "H plasma"), and the working gas of D_2 and the beam particle of the neutral beam of hydrogen (denoted as "D plasma").

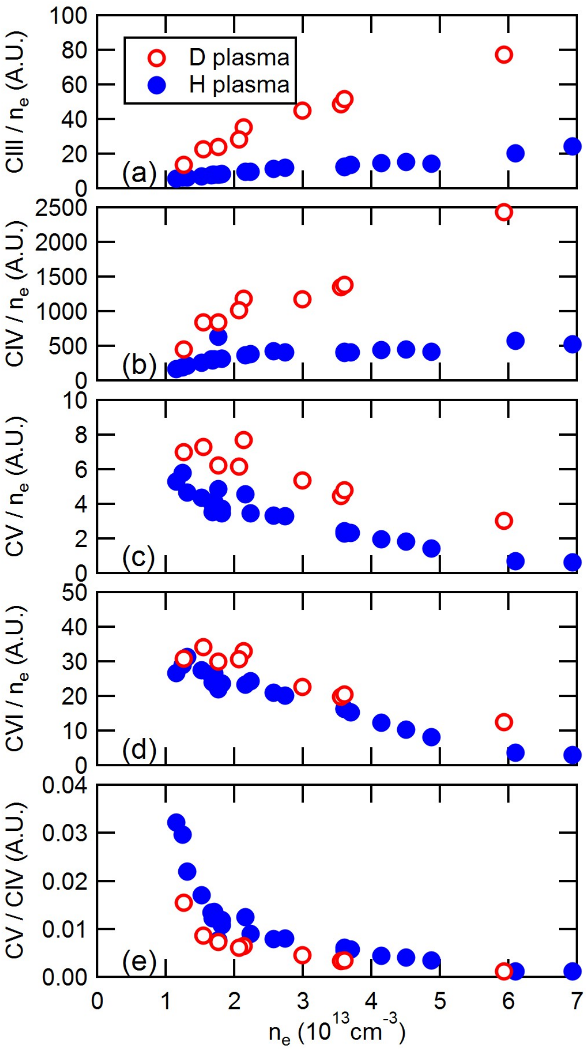

Fig. 1 Electron density dependence of line intensity of (a) CIII, (b) CIV, (c) CV, (d) CVI normalized by the electron density and (e) line ratio CV / CIV for deuterium and hydrogen discharges.

Intensities of carbon line emissions are monitored as an indicator of the impurity screening. CIII (977.03 Å, $2s^2$-2s2p) and CIV (1548.02 Å, 2s-2p) are measured using a 20 cm normal incidence VUV spectrometer [5], while CV (40.27 Å, $1s^2$-1s2p) and CVI (33.73 Å, 1s-2p) are measured using a grazing incidence EUV spectrometer [6]. The ionization potential, *E*i, for C^{2+}, C^{3+}, C^{4+}, and C^{5+} is 48 eV, 65 eV, 392 eV, and 490 eV, respectively. Therefore, CIII and CIV radiation is emitted by carbon ions with low *E*i located at the outer region of the ergodic layer, while CV and CVI radiation is emitted by carbon ions with high *E*i located at inner region of the ergodic layer. Figure 1 shows the electron density dependence of line intensity of (a) CIII, (b) CIV, (c) CV, and (d) CVI normalized by the line-averaged electron density and (e) a line ratio of CV / CIV as an indicator of the impurity screening effect. Smaller values of the ratio leads to enhancement of the impurity screening effect. The line ratio decreases with the electron density, because carbon lines emitted from the outer region of the ergodic layer (CIII, CIV) increase, while those from inner region (CV, CVI) decrease. It indicates enhancement of the impurity screening in the high density regime. Figure 1(e) also shows a comparison of the line ratio between the D plasmas compared to the H plasmas. The impurity screening effect is more obvious in the D plasmas. Enhancement of the friction force in D plasmas might be one of the reasons of the effective impurity screening.

Figure 2 shows vertical profiles at the bottom edge of the ergodic layer of the flow velocity derived from the CIV line emission measured by VUV spectroscopy for an H plasma and a D plasma with a magnetic configuration with R_{ax} = 3.6 m and B_t = 2.75 T. The observation range of the edge profile measurement of the VUV spectroscopy is shown in Fig. 2 [7]. The flow velocity along the sightline, v_R, is given by $v_R = c\,(\Delta\lambda\ /\ \lambda)$, where c is the light speed, $\Delta\lambda$ the Doppler-shift and λ the wavelength of line emission. The measured flow velocity is projection of the flow along the observation chord which can be approximately considered to be the direction of the plasma major radius. Therefore, a variable of v_R is used to indicate the measured flow value. Positive and negative sign in the vertical axis of Fig. 2 corresponds to the outboard an inboard direction along the plasma major radius, respectively. As shown in the figure, the flow velocity toward the outboard direction develops clearly with the maximum value at Z = -480 mm, which is a location close to the outermost region of the ergodic layer in the H plasma. This direction is same as the friction force in the parallel momentum balance calculated with a three-dimensional simulation code, EMC3-EIRENE [8]. On the other hand, the maximum value of the flow velocity in the D plasma is clearly smaller than that in the H plasma.

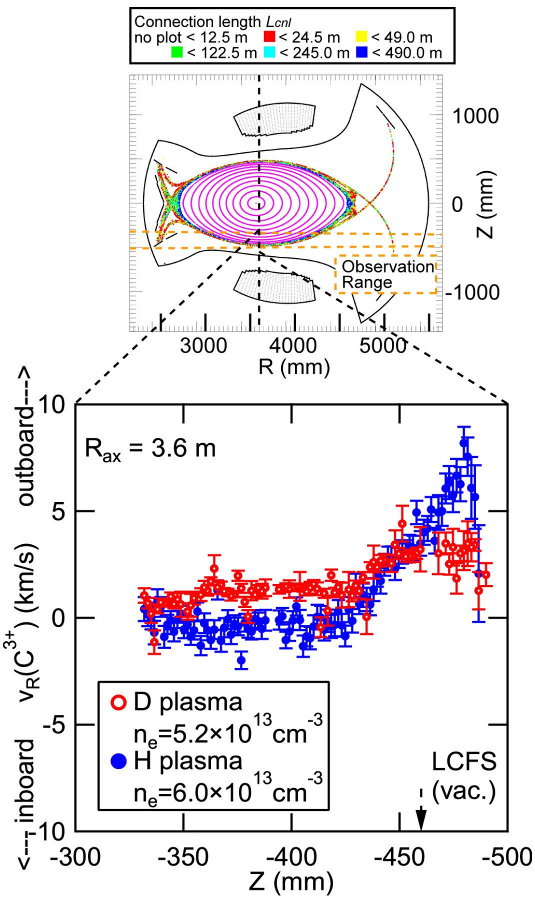

Fig. 2 Vertical profile at the bottom edge of the ergodic layer of impurity flow velocity derived from the Doppler profile of the CIV line emission measured by VUV spectroscopy in a D plasma (red open circle) and a H plasma (blue closed circle). The observation range of the VUV spectroscopy is illustrated together.

The electron density dependence of the maximum value of the observed flow is summarized in Fig. 3. All plots in the figure have directions same as the friction force. In the case of the H-discharge, the flow increases with the electron density. The result supports a prediction by the simulation that the friction force becomes more dominant in the force balance in higher density regime, which results in the increase of impurity flow causing the impurity screening. In the case of the D-discharge, the flow has a smaller value. In the friction force term in the equation of the momentum balance, $m_Z\ (V_{i//} - V_{Z//}^{imp})\ /\ \tau_s$, the parallel velocity of the bulk ion, $V_{i//}$, and the collision time between the bulk ion and the impurity ion, τ_s, might be changed between the H-discharge and the D-discharge. Further experiments and simulations for the H-D comparison are needed to clarify the difference.

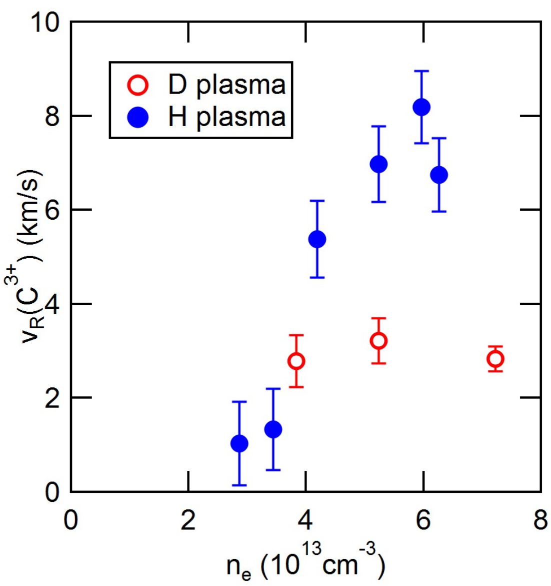

Fig. 3 Observed C^{3+} flow at the bottom edge of the ergodic layer in the H and D plasmas as a function of density for inward-shifted magnetic configuration with R_{ax} = 3.6 m.

The authors thank all the members of the LHD team for their cooperation with the LHD operation. This work is partially supported by the LHD project financial support (NIFS14ULPP010), and Grant-in-Aid for Young Scientists (B) (17K14426).

References

[1] T. Morisaki *et al.*, J. Nucl. Mater. **313-316** (2003) 548.
[2] M. B. Chowdhuri et *al.*, Phys. Plasmas **16** (2009) 062502.
[3] S. Morita *et al.*, Nucl. Fusion **53** (2013) 093017.
[4] M. Kobayashi *et al.*, Nucl. Fusion **53** (2013) 033011.
[5] T. Oishi *et al.*, Plasma Fus. Res. **10** (2015) 3402031.
[6] M. B. Chowdhuri *et al.*, Appl. Opt. **47** (2008) 135.
[7] T. Oishi *et al.*, Appl. Opt. **53** (2014) 6900.
[8] T. Oishi *et al.*, Nucl. Fusion **58** (2018) 016040.